Check for updates

Anterolateral Approach for Retrostyloid Superior Parapharyngeal Space Schwannomas Involving the Jugular Foramen Area: A 20-Year Experience

Sabino Luzzi[1,2], Alice Giotta Lucifero[1], Mattia Del Maestro[2,3], Giovanni Marfia[4,5], Stefania Elena Navone[4], Matias Baldoncini[6,7], Maximiliano Nuñez[8], Alvaro Campero[9,10], Samer K. Elbabaa[11], Renato Galzio[1,2]

■ BACKGROUND: **Schwannomas encompassing the superior parapharyngeal space are challenging lesions because of the anatomical complexity of this region and the frequent involvement of the neurovascular structures of the jugular foramen. The purpose of this study is to report the technical aspects and the advantages of the anterolateral approach, here proposed for schwannomas of this complex area.**

■ METHODS: **The main steps of the anterolateral approach are described in detail, along with the results of a consecutive series of 38 patients with a retrostyloid superior parapharyngeal schwannoma involving the jugular foramen operated on by means of this route between 1999 and 2019.**

■ RESULTS: **The supine position is generally preferred. The medial border of the sternocleidomastoid muscle, mastoid tip, and superior nuchal line are the landmarks for the hockey-stick skin incision. The accessory nerve is retrieved and mobilized cranially. Detachment of the sternocleidomastoid, digastric, and nuchal muscles allows for a 180° exposure of the extracranial side of the jugular foramen. Three working corridors, namely the pre-carotid, pre-jugular, and retro-jugular, allow access to the deeper part of the jugular foramen area and the superior parapharyngeal space. In the present series, a gross total resection was achieved in 89.4% of the patients. Three recurrences occurred after an average follow-up of 80.5 $\pm$ 51 months.**

■ CONCLUSIONS: **The anterolateral approach is highly effective in the treatment of retrostyloid superior parapharyngeal space schwannomas involving the jugular foramen. Its simplicity of execution, versatility, and very low morbidity are among its main strengths.**

INTRODUCTION

The parapharyngeal space (PPS) is classically divided into a superior, middle, and inferior compartment, but also a prestyloid and retrostyloid area (Figure 1), with regard to planning and tailoring the surgical approaches to this formidable area.[1,2] The PPS is involved in 45% of all schwannomas affecting the head and neck.[3] Schwannomas in this region may arise from the lower cranial nerves (LCNs), the sympathetic chain, or the peripheral nerve sheath, with the suprahyoid location being the most frequent.[4]

Key words
- Anterolateral approach
- Glossopharyngeal nerve diseases
- Jugular foramen tumors
- Lower cranial nerves
- Parapharyngeal space
- Schwannoma
- Skull base neoplasms

Abbreviations and Acronyms
ALA: Anterolateral approach
CT: Computed tomography
ICA: Internal carotid artery
IJV: Internal jugular vein
JF: Jugular foramen
LCN: Lower cranial nerve
MRI: Magnetic resonance imaging
PPS: Parapharyngeal space
VA: Vertebral artery

From the [1]Neurosurgery Unit, Department of Clinical-Surgical, Diagnostic and Pediatric Sciences, University of Pavia; [2]Neurosurgery Unit, Department of Surgical Sciences, Fondazione IRCCS Policlinico San Matteo; [3]PhD School in Experimental Medicine, Department of Clinical-Surgical, Diagnostic and Pediatric Sciences, University of Pavia, Pavia; [4]Experimental Neurosurgery and Cell Therapy Laboratory, Neurosurgery Unit, Fondazione IRCCS Ca'Granda Ospedale Maggiore Policlinico di Milano, Milan; [5]Institute of Aerospace Medicine, Italian Air Force, Milan, Italy; [6]Microsurgical Neuroanatomy Laboratory-LaNeMic- II Division of Anatomy, Medicine School, University of Buenos Aires; [7]Department of Neurological Surgery, San Fernando Hospital; [8] Department of Neurosurgery, Hospital El Cruce, Buenos Aires; [9]Servicio de Neurocirugía, Universidad Nacional de Tucumán; [10]Department of Neurosurgery, Hospital Padilla, San Miguel de Tucumán, Tucumán, Argentina; and [11]Pediatric Neurosurgery, Pediatric Neuroscience Center of Excellence, Arnold Palmer Hospital for Children, Orlando, Florida, USA

*To whom correspondence should be addressed: Sabino Luzzi, M.D., Ph.D.
[E-mail: sabino.luzzi@unipv.it]*

*Citation: World Neurosurg. (2019) 132:e40-e52.
https://doi.org/10.1016/j.wneu.2019.09.006*

Journal homepage: www.journals.elsevier.com/world-neurosurgery

Available online: www.sciencedirect.com

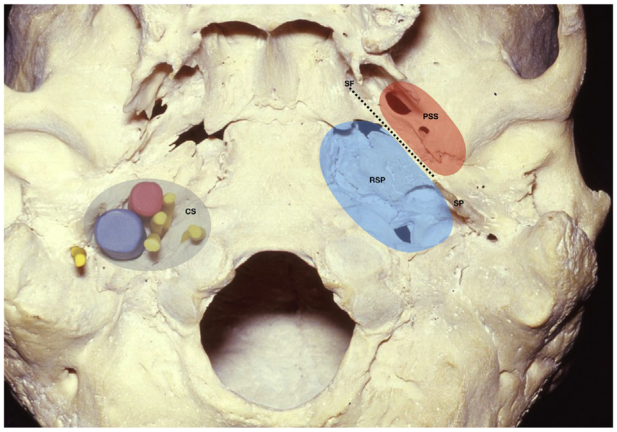

Figure 1. Parapharyngeal space. Gray area: carotid space; blue area: retrostyloid space; red area: prestyloid space. CS, carotid space; PSS, prestyloid space; RSS, retrostyloid space; SF, scaphoid fossa of the sphenoid bone; SP, styloid process.

Cervical schwannomas arising from the LCNs generally grow within the retrostyloid PPS; may involve superiorly the infratemporal fossa; compress and displace the carotid, prevertebral, masticator, and parotid spaces; and pose special issues because of their intimate relationship with the neurovascular structures of the jugular foramen (JF) area. Radical surgery is the cure for these lesions but requires full exposure of the mass that unavoidably leads to additional problems when dealing with the JF.

Both cervical and skull base approaches have been reported for the treatment of schwannomas located within this area; however, the former is limited in the exposure of the superior PPS and the latter is burdened by a high morbidity.[5-17]

Although lateral skull base approaches to the superior PPS and the infratemporal fossa are widely preferred to the anterior and the inferior approaches, they entail by default, for example, for the Fisch type A approach, a conductive hearing loss and a facial numbness secondary to the anterior transposition of the facial nerve; these complications are difficult to accept for the treatment of benign tumors such as schwannomas. As a consequence, lateral infratemporal fossa approaches are indicated for dumbbell lesions rather than for those with a minimal involvement of the JF area, as in the majority of the retrostyloid superior PPS schwannomas.[13,15,18,19]

An "anterolateral approach" (ALA) to the craniovertebral junction for the treatment of anterior extradural foramen magnum meningiomas and peripheral nerve sheath schwannomas was described by Bernard George in the 1980s.[20-24]

At that time Lesoin also highlighted the advantages of the ALA in the management of primary and secondary bone tumors and traumas.[25-28]

Providing a full and direct exposure of the extracranial side of the JF and the superior PPS, as well as the atlantic segment of the extradural vertebral artery (VA), with no need for hearing sacrifice, rerouting of the facial nerve, or infralabyrinthine bony exposure, the ALA also represents an effective and elegant corridor to the upper retrostyloid compartment and to all those primary or secondary lesions involving the extracranial side of the JF area. Further strengths of the ALA are its relatively simple execution, its effectiveness in allowing for a gross total tumor removal, and its very low morbidity. It also allows the possibility of performing a posteromedial transposition of the VA and posteriorly widening the working corridor.

To highlight the advantages of the ALA in allowing total tumor removal with a very low morbidity, we report the retrospective results of a 20-year case series of the surgical management of retrostyloid superior parapharyngeal space schwannomas involving the jugular foramen area. Additional conclusions from this large series include the incidence of parapharyngeal schwannomas according to their origin from the different LCNs, and the frequency of the involvement of the different PPS compartments.

MATERIALS AND METHODS

The study has been approved by our Internal Advisory Board. Data regarding 38 retrostyloid schwannomas consecutively operated on by means of an ALA have been retrospectively reviewed. The incidence according to the origin from the LCNs, involvement of the different PPS compartments, average tumor volume, surgical technique, extent of resection, and outcome were the parameters analyzed in more detail. Preoperative imaging workup consisted of conventional multiplanar cervical computed tomography (CT) and gadolinium contrast-enhanced magnetic resonance imaging (MRI), both extended upward to involve the craniovertebral junction. Tumor volume was calculated with a medical imaging workstation (Osirix DICOM Viewer; Pixmeo, Bernex, Switzerland) based on MRI for each patient. All of the patients had undergone a CT angiography and a time-of-flight magnetic resonance angiography, the latter in arterial and venous phases. The need for digital subtraction angiography was decided on a case-by-case basis. Apart from the first 6 cases dating back to before 2010, all of the patients have undergone intraoperative neuromonitoring of the VII and IX to XII cranial nerves, which involved free-running and direct stimulation techniques. For the vagus nerve, a laryngotracheal tube with imbedded electrodes was preferred. Surgeries were performed by the senior author (RG) in 3 different Italian hospitals between January 1999 and June 2019.

RESULTS

Incidence and Volume of Parapharyngeal Schwannomas According to Their Origin from the LCNs

Among the LCNs, the glossopharyngeal nerve was the most frequently affected (47%), followed by the vagus nerve (31%). Hypoglossal schwannomas and schwannomas arising from the sympathetic chain were extremely rare. No accessory nerve schwannomas occurred in the present series (Figure 2). The overall average schwannoma volume was 27.1 ± 27 cm^3. The average schwannoma volume was 27.1 ± 3, 27.3, 26.3 ± 2, and 22.1 ± 5 cm^3 for tumors arising from the glossopharyngeal, vagus, and hypoglossal nerves and the sympathetic chain, respectively (Table 1).

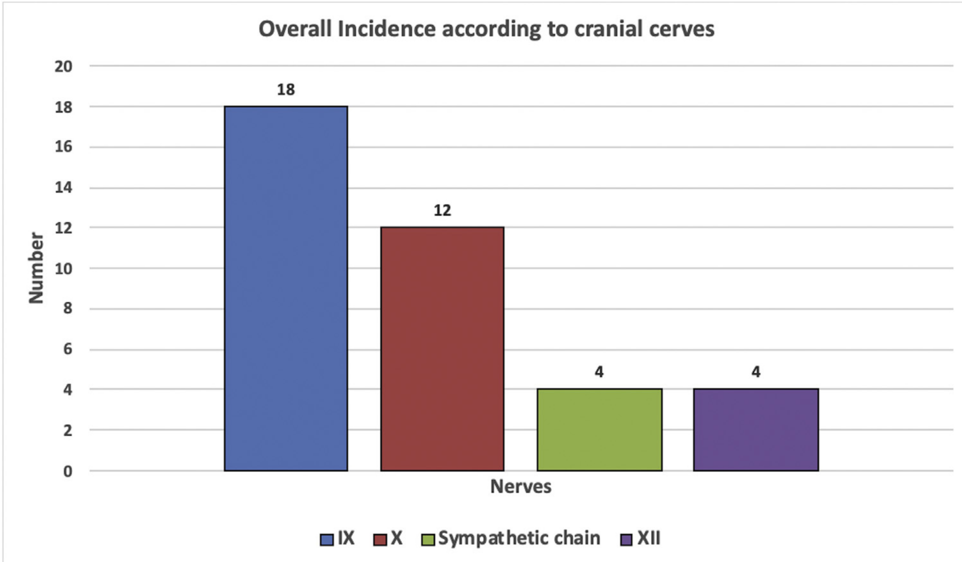

Figure 2. Bar graph showing the incidence of parapharyngeal schwannomas according to their origin from the lower cranial nerves and the sympathetic chain. IX, glossopharyngeal nerve; X, vagus nerve; XII, hypoglossal nerve.

Involvement of Different Parapharyngeal Space Compartments

The superior PPS compartment was involved in 81.5% of the total cases. Within the "superior" group, the extracranial side of the JF was involved in 80% of the patients, whereas more than a single compartment was involved in 28% of the lesions (Figure 3).

Schwannomas arising from the sympathetic chain tended to have the longest craniocaudal pattern of growth and thus were often multicompartmental. A dumbbell growth was seen in 2 schwannomas where a cervical stage was performed through the ALA. In one case, the patient underwent a further, delayed, far-lateral paracondylar approach to complete the removal of a large remnant. In the other case, the extent of the resection was subtotal, and a wait-and-see policy was adopted.

Technical Aspects of the Anterolateral Approach

Positioning and Identification of the Surface Landmarks. The patient is placed supine with the thorax rotated 20° toward the opposite side and the head fixed with a Mayfield-Kees skull clamp, which is generally preferred to a Sugita headrest because it is less bulky. To promote venous return from the internal jugular vein (IJV), and to facilitate the identification and decompression of the VA, the head is rotated 25° toward the nonaffected side and extended 5° (Figure 4). The recognition of the main landmarks, namely the cricoid cartilage of the larynx, the mastoid tip, and the medial border of the sternocleidomastoid muscle and the superior nuchal line, is a paramount step for orientation. Before the skin incision, we usually perform a subcutaneous infiltration with two 5-mL vials of mepivacaine hydrochloride 1% (20 mg/mL) and normal saline 9% (dilution 1:1).

Skin Incision. The skin incision basically has a hockey-stick shape. It starts in the nuchal region, at the level of the superior nuchal line, descends laterally and downward to reach the medial border of the sternocleidomastoid muscle passing above the mastoid tip, and stops at the level of the cricoid cartilage of the larynx. The skin incision can be extended inferiorly as needed, which is often the case for lesions extending inferiorly to the infrahyoid space (Figure 5).

Skeletonization of the Extracranial Side of the Jugular Foramen and the Retrostyloid Parapharyngeal Space. The trapezius and platysma muscles are initially identified. The platysma is cut longitudinally just in front of the medial border of the sternocleidomastoid muscle to allow for a pre-sternocleidomastoid access route. After the incision of the middle cervical fascia, the dissection proceeds between the lateral border of the IJV and the medial surface of the sternocleidomastoid muscle. Here it is mandatory to identify the spinal accessory nerve, which enters the medial surface of the sternocleidomastoid muscle at the upper third level. The nerve is directed posteriorly, crossing the IJV. The accessory nerve has to be retrieved and mobilized cranially, with its fat envelope kept intact around it in order to avoid damage. In this phase, a direct stimulation of the nerve may be useful for its identification. The dissection becomes subperiosteal to the mastoid tip, where the sternocleidomastoid and the posterior belly of the digastric muscle are detached to complete the skeletonization of the occipitomastoid area and the C1 transverse process with the VA. A posteromedial en-bloc mobilization of the nuchal muscles is required to allow for a 180° exposure of the lateral aspect of the extracranial side of the JF area, as well as of all the related neurovascular

Table 1. Overall Data About Demographics, Clinical-Radiological Findings, and Surgical and Clinical Outcome of 38 Patients Harboring a Retrostyloid Superior Parapharyngeal Space Schwannoma Who Underwent an Anterolateral Approach

						Anatomical Relationship with JF						
Patient No.	Sex	Age	Tumor Origin	Tumor Volume (cm^3)	PPS Compartment	Involvement of EJF	Pattern of Growth	Clinical Onset	Complications	Extent of Resection	Follow-Up (Months)	Recurrences
1	F	28	IX	28.8	Upper	Yes	Dumbbell	Glossopharyngeal neuralgia, swallowing	None	GTR	180	No
2	M	47	Sympatetic chain	19.7	Middle	No	Extracranial	Cervical solid mass	None	GTR	70	No
3	F	67	X	12.2	Upper	Yes	Extracranial	Bitonal voice	None	GTR	3	No
4	F	32	XII	24.1	Upper	Yes	Extracranial	Hemitongue atrophy	None	GTR	85	No
5	M	37	X	9.5	Upper	Yes	Extracranial	Cervical solid mass	None	GTR	90	No
6	M	25	IX	4.5	Middle	No	Extracranial	Incidental	Swallowing recovered within 6 months	GTR	32	No
7	M	48	Sympatetic chain	11.7	Upper + middle	No	Extracranial	Cervical solid mass, bitonal voice	None	GTR	210	Yes
8	F	57	IX	25.7	Upper	Yes	Extracranial	Incidental	None	GTR	120	No
9	M	52	IX	21.2	Upper	Yes	Extracranial	Dysphagia, hoarseness	None	STR	12	No
10	F	70	IX	58.1	Upper + middle	Yes	Extracranial	Pharyngeal solid mass	None	GTR	14	No
11	M	46	Sympatetic chain	10.8	Upper	Yes	Extracranial	Cervical solid mass, bitonal voice	None	GTR	90	No
12	F	60	XII	4.5	Upper	Yes	Extracranial	Incidental	None	GTR	35	Yes
13	F	65	X	8.3	Middle	No	Extracranial	Swallowing, cough	None	GTR	56	No
14	M	33	IX	12.2	Middle	No	Extracranial	Glossopharyngeal neuralgia	None	GTR	80	No
15	F	50	IX	27.2	Middle	No	Extracranial	Pharyngeal solid mass	None	GTR	130	No
16	F	67	X	7.6	Upper	No	Extracranial	Bitonal voice	None	GTR	88	No
17	F	31	IX	25.7	Upper	Yes	Dumbbell	Swallowing, dysphonia	None	STR	140	Yes
18	M	77	X	3.8	Upper	Yes	Extracranial	Incidental	Hemidiaphragm paralysis, dysphagia, need for jejunostomy	GTR	127	No
19	F	49	IX	24.1	Upper + middle	No	Extracranial	Cervical solid mass	None	STR	36	No
20	M	63	X	4.5	Upper	No	Extracranial	Dysphagia, dysphonia	Vocal cord paralysis, bitonal voice	GTR	115	No
21	F	53	X	6.2	Upper	Yes	Extracranial	Dysphagia	None	GTR	100	No

EJF, extracranial side of jugular foramen; F, female; GTR, gross total resection; IX, glossopharyngeal nerve; JF, jugular foramen; M, male; PPS, parapharyngeal space; STR, subtotal resection; X, vagus nerve; XII, hypoglossal nerve.

Continues

Table 1. Continued

Patient No.	Sex	Age	Tumor Origin	Tumor Volume (cm^3)	PPS Compartment	Anatomical Relationship with JF: Involvement of EJF	Anatomical Relationship with JF: Pattern of Growth	Clinical Onset	Complications	Extent of Resection	Follow-Up (Months)	Recurrences
22	M	34	IX	12.2	Middle	No	Extracranial	Glossopharyngeal neuralgia	None	GTR	70	No
23	F	31	X	72	Upper + middle	Yes	Extracranial	Horner's syndrome, cough	None	GTR	140	No
24	F	52	Sympatetic chain	103.3	Upper + middle+ lower	Yes	Extracranial	Cervical solid mass, neck pain, bitonal voice	None	GTR	12	No
25	M	30	IX	9.5	Upper	Yes	Extracranial	Hoarseness	None	GTR	130	No
26	M	37	X	28.9	Middle	No	Extracranial	Cervical solid mass	Bitonal voice	GTR	8	No
27	F	79	IX	58.1	Upper +middle	Yes	Extracranial	Glossopharyngeal neuralgia	None	STR	112	No
28	M	31	IX	13.5	Upper	Yes	Extracranial	Glossopharyngeal neuralgia, pharyngeal solid mass	None	GTR	60	No
29	M	71	XII	22.5	Upper	Yes	Extracranial	Incidental	Hemitongue atrophy	GTR	75	No
30	F	44	IX	10.8	Upper	Yes	Extracranial	Cough	None	GTR	80	No
31	M	47	IX	90.3	Upper + middle	Yes	Extracranial	Dysphagia, hoarseness	None	GTR	6	No
32	F	55	XII	52.6	Upper + middle	Yes	Extracranial	Hemitongue atrophy	None	GTR	100	No
33	M	29	X	13.5	Upper	No	Extracranial	Dysphagia, hoarseness, dysphonia	None	GTR	24	No
34	F	38	IX	7.6	Upper	Yes	Extracranial	Neck pain, hoarseness	Dysphagia recovered after 2 months	GTR	66	No
35	F	41	X	44.7	Upper + middle	Yes	Extracranial	Bitonal voice	None	GTR	28	No
36	M	19	IX	103.9	Upper + middle+ lower	No	Extracranial	Dysphagia, swallowing	None	GTR	86	No
37	M	42	IX	24	Upper	Yes	Extracranial	Incidental	None	GTR	90	No
38	F	56	X	11.7	Upper	Yes	Extracranial	Neck pain	None	GTR	160	No

EJF, extracranial side of jugular foramen; F, female; GTR, gross total resection; IX, glossopharyngeal nerve; JF, jugular foramen; M, male; PPS, parapharyngeal space; STR, subtotal resection; X, vagus nerve; XII, hypoglossal nerve.

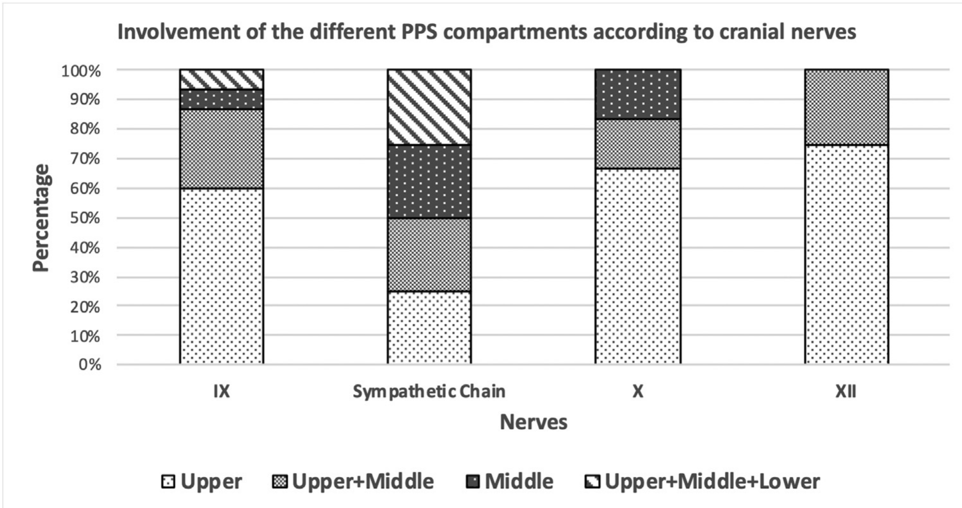

Figure 3. Bar graph showing the involvement of the different parapharyngeal compartments according to the cranial nerves. IX, glossopharyngeal nerve; PPS, parapharyngeal space; X, vagus nerve; XII, hypoglossal nerve.

structures running within the retrostyloid compartment of the superior PPS.

Identification of the Working Corridors

Pre-Carotid Corridor. The pre-carotid corridor is bounded anteriorly by the styloid diaphragm and the so-called aponeurosis of Zuckerkandl and Testut (stylopharyngeal fascia) and posteriorly by the anterior wall of the internal carotid artery (ICA). The roof of this corridor is formed by the stylomastoid process, the stylomastoid foramen, and the common trunk of the facial nerve before it splits into its 5 major parotid branches. The floor blends inferiorly in the carotid triangle (Figure 6).

Pre-Jugular Corridor. The back wall of the ICA and the anterior wall of the IJV represent the anterior and the posterior limit, respectively, of this corridor, whereas the roof is constituted medially by the extracranial side of the JF with all of the related neurovascular structures and laterally by the mastoid tip (Figure 7).

Figure 4. Patient position for the anterolateral approach.

Figure 5. Identification of the surface landmarks for the anterolateral approach, namely the medial border of the sternocleidomastoid muscle, superior nuchal line, mastoid tip, and cricoid cartilage of the larynx. Planning of the hockey-stick—shaped skin incision.

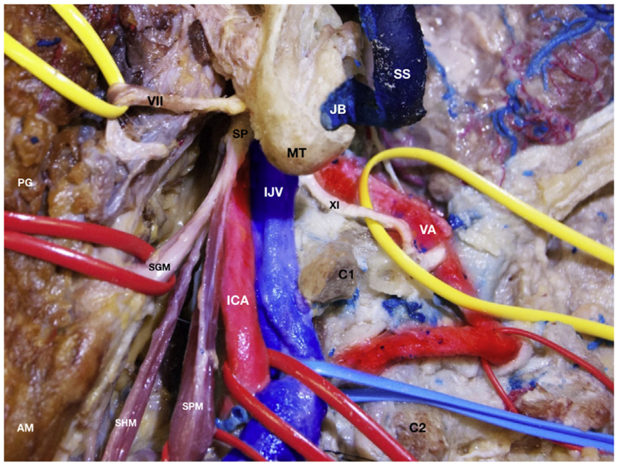

Figure 6. Anatomic cadaveric dissection of the superior retrostyloid parapharyngeal space and jugular foramen region at the extracranial side. The head has been formalin-fixed, and the vessels have been injected with colored silicone (red for arteries and blue for veins). The vertebral artery has been released from the C1 transverse process and transposed posteromedially. AM, angle of the mandible; C1, atlas; C2, axis; ICA, internal carotid artery; IJV, internal jugular vein; JB, jugular bulb; MT, mastoid tip; PG, parotid gland; SGM, styloglossus muscle; SHM, stylohyoid muscle; SP, styloid process; SPM, stylopharyngeal muscle; SS, sigmoid sinus; VA, vertebral artery; VII, facial nerve; XI, accessory nerve.

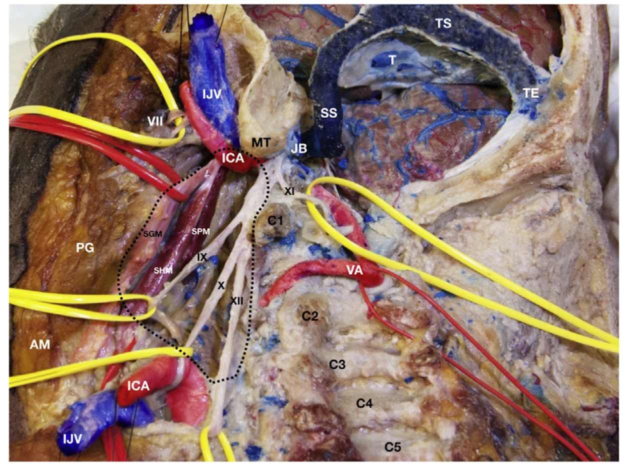

Figure 7. Further anatomic cadaveric dissection of the superior retrostyloid parapharyngeal space and jugular foramen region at the extracranial side where the internal carotid artery and the internal jugular vein have been cut and reflected to expose the cranial nerves exiting from the jugular foramen. *Dotted line* indicates the retrostyloid space lying behind the styloid diaphragm. AM, angle of the mandible; C1, atlas; C2, axis; C3, third cervical vertebra; C4, fourth cervical vertebra; C5, fifth cervical vertebra; ICA, internal carotid artery; IJV, internal jugular vein; IX, glossopharyngeal nerve; JB, jugular bulb; MT, mastoid tip; PG, parotid gland; SGM, styloglossus muscle; SHM, stylohyoid muscle; SP, styloid process; SPM, stylopharyngeal muscle; SS, sigmoid sinus; T, tentorium; TE, torcular Herophili; TS, transverse sinus; VA, vertebral artery; VII, facial nerve; X, vagus nerve; XI, accessory nerve; XII, hypoglossal nerve.

Retro-Jugular (Prevertebral Artery) Corridor. The narrowed retro-jugular corridor is limited anteriorly by the back wall of the IJV and posteriorly by the C1 transverse process hosting the V3 foraminal segment of the atlantal part of the VA.[29] The jugular bulb forms the roof of this area. The distance between the mastoid tip and the sagittal segment of the VA and between the mastoid tip and the C1 transverse process measures 21 and 19.6 mm, respectively[30] (**Figure 8**). This distance indicates the theoretical width of this corridor, which can be widened only by means of a posteromedial transposition of the VA after the C1 transverse process is unroofed. Such a posterior extension of the ALA allows for a 270° exposure of the extracranial side of the JF area (**Figure 9**).

Tumor Excision. Conventional microneurosurgical techniques are generally employed for schwannoma excision. Magnification and illumination of the surgical field provided by the surgical microscope allow for a careful dissection of all of the neurovascular structures involved by the mass. Sharp dissection to release vessels and nerves in case of encasement is paramount. The main steps for schwannoma excision include a full exposure of the tumor, including the superior and the inferior poles, a capsular incision, an inside-out debulking, the identification of the interface between the mass and the normal nerve bundle, and, finally, the tumor removal. Meticulous hemostasis with both bipolar coagulation and hemostatic materials ought to be avoided because it is potentially dangerous for the residual nerve trunk.

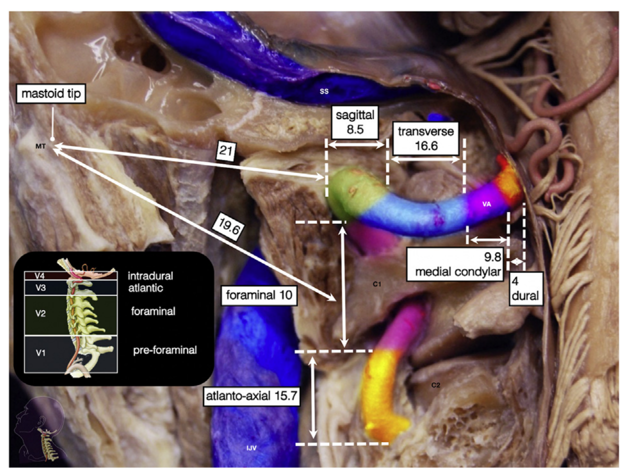

Figure 8. Anatomic cadaveric dissection of the condylar and the paracondylar region showing the distance between the mastoid tip and the sagittal segment of the atlantic part of the vertebral artery (21 mm) and the mastoid tip and the C1 transverse process (19.6 mm). The black panel shows the different segments of the vertebral artery, whereas the subsegments of the V3 atlantic part have been reported in different colors. The length of each subsegment has been reported. C1, atlas; C2, axis; IJV, internal jugular vein; MT, mastoid tip; SS, sigmoid sinus; VA, vertebral artery.

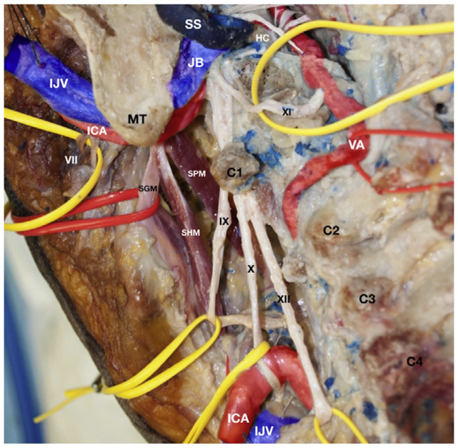

Figure 9. Anatomic cadaveric dissection of the condylar and paracondylar region from a posterior retro-jugular perspective. The hypoglossal canal has been skeletonized. A lateral partial condylectomy and a posteromedial transposition of the vertebral artery have also been performed to enlarge the retro-jugular corridor to the extracranial side of the jugular foramen and retrostyloid parapharyngeal space. C1, atlas; C2, axis; C3, third cervical vertebra; C4, fourth cervical vertebra; HC, hypoglossal canal; ICA, internal carotid artery; IJV, internal jugular vein; IX, glossopharyngeal nerve; JB, jugular bulb; MT, mastoid tip; SGM, styloglossus muscle; SHM, stylohyoid muscle; SPM, stylopharyngeal muscle; SS, sigmoid sinus; VA, vertebral artery; VII, facial nerve; X, vagus nerve; XI, accessory nerve; XII, hypoglossal nerve.

Closure. The middle cervical fascia is sutured, and a submuscular drain can be positioned at this step. The platysma muscle is also sutured before proceeding to the subcuticular and skin closure.

The overall operative time for the approach is approximately 60 minutes.

Illustrative Cases

Case 1. Superior Parapharyngeal Retrostyloid Schwannoma Involving the Jugular Foramen: Combined Pre-Jugular/Retro-Jugular Corridor. Because of a persistent glossopharyngeal neuralgia, a 31-year-old man underwent a contrast-enhanced MRI that revealed a left retrostyloid schwannoma with a partial involvement of the neurovascular structures of the JF (Figure 10A). Magnetic resonance angiography clearly documented an anterior displacement of the ICA with a subsequent enlargement of the pre-jugular corridor (Figure 10B and C). The patient underwent an ALA aimed at exploiting the widened pre-jugular corridor, but the tenacious adhesions of the mass to the jugular bulb and the other LCNs made a combined pre-jugular/retro-jugular corridor necessary (Figure 10D). A posteromedial transposition of the VA was performed; this posterolateral extension of the approach allowed a safe and effective excision of residual tumor just below the jugular bulb (Figure 10E and F). The posterior corridor also facilitated the confirmation of the origin of the tumor from the glossopharyngeal nerve as well as the recognition of the remaining cranial nerves. The patient was discharged on the second postoperative day neurologically intact (Figure 10G and H). MRI confirmed the complete excision of the tumor (Figure 10I).

Case 2. Extracranial Jugular Foramen Schwannoma Extending into the Retrostyloid Space: Direct Lateral Approach Through a Single Pre-Jugular Corridor. A 57-year-old woman underwent a CT scan because of a mild traumatic head injury. Incidentally, a round solid mass was found at the extracranial side of the left JF. Contrast-enhanced MRI and CT angiography documented a schwannoma located in the retrostyloid compartment of the superior PPS (Figure 11A). The ICA appeared to be anteriorly displaced but not encased (Figure 11B–E). An ALA was used (Figure 11F); the pre-jugular corridor was used for approach as it was already enlarged by the lesion, which appeared to originate from the glossopharyngeal nerve just below the JF (Figure 11G). A gross total removal was possible with no complications and no recurrences at 120 months (Figure 11H).

Case 3. Retrostyloid Schwannoma Involving the Prevertebral Space: Retro-Jugular Corridor and Handling of the Atlanto-Axial Segment of the Vertebral Artery. A young woman who suffered from a long history of neck pain and hoarseness underwent a contrast-enhanced MRI of the head. A left, round-shaped, retrostyloid superior PPS schwannoma was detected (Figure 12A and B). An anterolateral retro-jugular approach was used. The VA was transposed posteriorly, creating a wider corridor that allowed for an early release of the artery from the mass, as well as gross total removal of the tumor. Postoperatively, the patient had a transient paradoxical dysphagia from which she appeared completely recovered after 2 months. MRI showed no tumor recurrence at 66-month follow-up (Figure 12C and D).

Case 4. Large Multicompartmental Schwannoma Involving the Jugular Foramen: Multicorridor Anterolateral Approach. A 52-year-old woman with a large right solid cervical mass had a tumor involving the entire PPS as well as the carotid, parotid, and prevertebral spaces diagnosed (Figure 13A). Symptomatology included a long history of neck pain and the more recent appearance of bitonal voice. A partial encasement of the ICA and the IJV was also revealed (Figure 13B and C). Furthermore, the IJV was severely compressed and shifted posteriorly (Figure 13D). A fine-needle aspiration biopsy allowed conclusive diagnosis of a schwannoma. An ALA, extended below to also involve the infrahyoid compartment, was planned. In this case, all 3 working corridors were essential to achieve a gross total removal of the tumor, which was particularly difficult at the level of the extracranial JF. Intraoperatively, the tumor appeared to arise from the sympathetic chain. The patient was discharged 3 days after surgery, and no recurrences have been documented at 12-month follow-up (Figure 13E and F).

Extent of Resection

A gross total resection was achieved for 89.4% of the tumors.

Approach-Related Complications

No approach-related complications occurred in the present series.

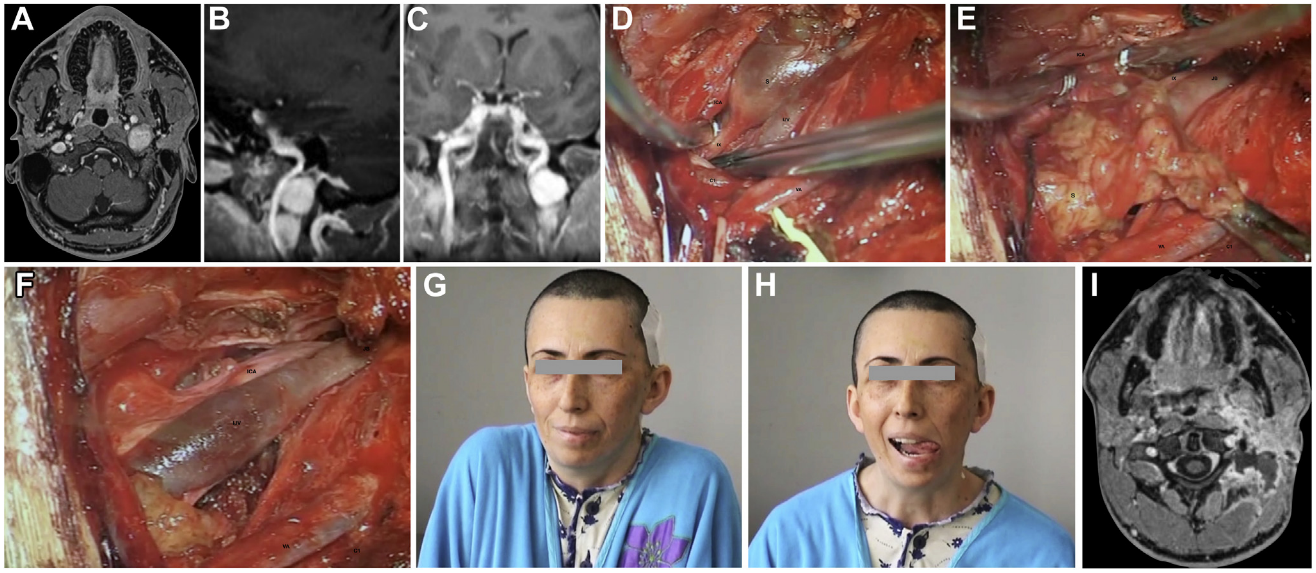

Figure 10. (**A**) Axial gadolinium contrast-enhanced T1-weighted MRI image revealing a left retrostyloid schwannoma with a partial involvement of the neurovascular structures of the jugular foramen. (**B**) Sagittal and (**C**) axial MR angiography showing the anterior displacement of the internal carotid artery with the enlargement of the pre-jugular corridor. (**D**–**F**) Operative photograph illustrating the pre-jugular corridor widened by the mass. A combined pre-jugular/retro-jugular corridor allowed for a gross total tumor removal. (**G, H**) Second postoperative day photograph of the patient who was neurologically intact. (**I**) Axial gadolinium contrast-enhanced T1-weighted MRI image confirming the gross total resection of the tumor. C1, atlas; ICA, internal carotid artery; IJV, internal jugular vein; IX, glossopharyngeal nerve; JB, jugular bulb; MRI, magnetic resonance imaging; S, schwannoma; VA, vertebral artery.

Clinical Outcome

Six patients (15.7%) suffered from postoperative sequelae. Among these cases, 3 tumors originated from the vagus nerve, 2 from the glossopharyngeal nerve, and 1 from the hypoglossal nerve (Table 1).

Recurrence Rate

Three recurrences occurred during an average follow-up of 80.5 ± 51 months. In one of these cases, the excision of the tumor had been partial.

DISCUSSION

In recent years, new insights into the molecular mechanisms underlying familiar and sporadic forms of schwannomas as well as other pathologies affecting the central nervous system have been gained.[31-44]

Despite these advances, there is still no therapy other than surgery that is considered to be a cure for these tumors. The PPS and the JF regions are classically considered complicated areas to deal with because the vital neurovascular structures involved and the narrowness of the spaces make surgery challenging. A wide spectrum of tumors, including schwannomas, affects these well-defined anatomical compartments, and many have a multi-compartmental extension.

Several approaches have been reported for both the superior PPS and the extracranial JF area, each of which has advantages and disadvantages. Nevertheless, very few of them allow for a concurrent combined handling of the major cervical vessels and the LCNs in their entire cervical extension. Classic ear, nose and throat and maxillofacial approaches, such as the transcervical, transparotid, transmandibular, transmastoid, transmaxillary, transoral, or a combination of these, are limited in the presence of an extensive skull base involvement.[19]

In particular, among the anterior transfacial corridors, the maxillary swing approach is burdened by disabling complications, such as facial scarring, palatal insufficiency eustachian tube dysfunction, and cheek anesthesia.[45]

Mandibulotomy is associated with malocclusion, mandibular anesthesia, mental nerve damage, and delayed wound healing.[5,18,19]

The transoral corridors are associated with an unacceptable risk of infections. As a consequence, lateral skull base approaches, primarily Fisch's infratemporal fossa approach, have become elective for all those extracranial tumors that involve the jugular and the stylomastoid foramen, the foramen ovale, and the petrous and lacerum segments of the ICA.[46] Type A to D infratemporal fossa approaches allow for an unparalleled handling of the PPS and the petrous segment of the ICA. However, they are characterized by dramatic morbidity, including facial nerve palsy secondary to the permanent anterior transposition of the facial nerve and conductive hearing loss, both falling under the type A infratemporal fossa approach.

The main advantages of the ALA are ease of performance, full and concurrent exposure of both the PPS and the extracranial side of the JF, early control of the V3 segment of the VA, high versatility

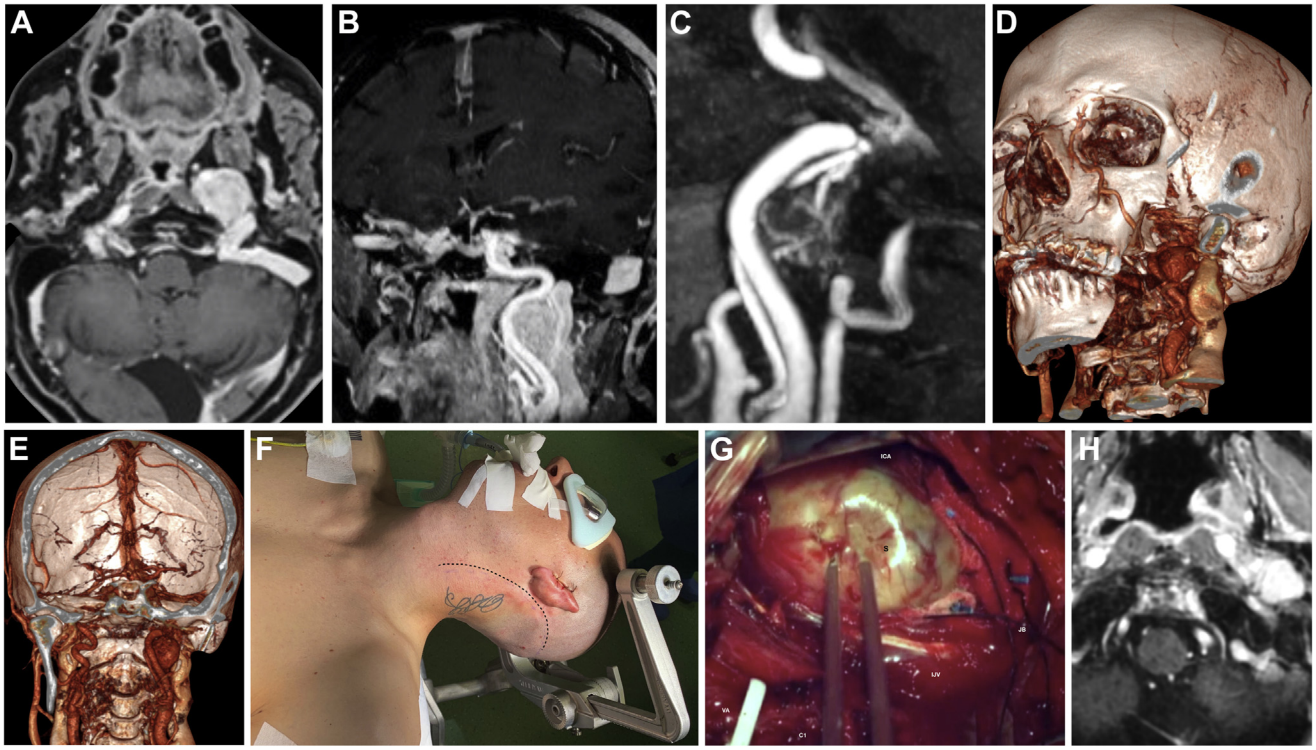

Figure 11. (**A**) Axial gadolinium contrast-enhanced T1-weighted MRI image showing a schwannoma located in the retrostyloid compartment of the superior parapharyngeal space. (**B**) Coronal and (**C**) sagittal MRI angiography revealing the anterior displacement of the internal carotid artery. (**D**) Oblique and (**E**) coronal view of 3D CT angiography documenting the anatomical relationship of the mass with the jugular foramen region, along with the enlargement of the pre-jugular corridor. (**F**) Patient position for the left anterolateral approach. (**G**) Operative photograph showing the enlarged pre-jugular corridor. The same corridor was used to approach the lesion, which appeared to originate from the glossopharyngeal nerve. (**H**) Axial gadolinium contrast-enhanced T1-weighted postoperative MRI image documenting the total removal of the lesion and the restoration of the normal caliber of the left dominant internal jugular vein. C1, atlas; CT, computed tomography; ICA, internal carotid artery; IJV, internal jugular vein; JB, jugular bulb; MRI, magnetic resonance imaging; S, schwannoma; VA, vertebral artery.

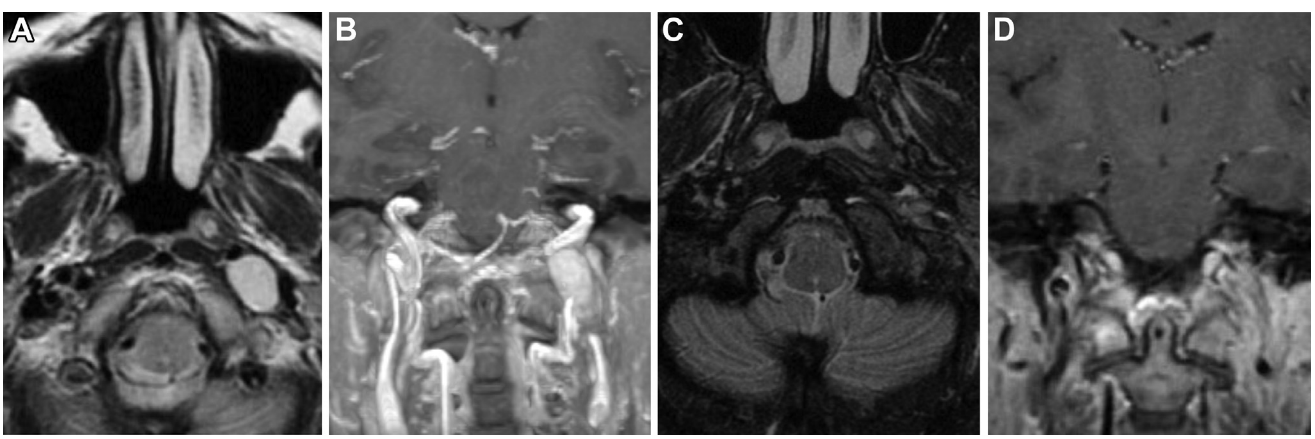

Figure 12. (**A**) Axial T1-weighted MRI image revealing a left retrostyloid schwannoma involving the extracranial side of the jugular foramen. (**B**) Coronal MRI angiography showing the intimate relationship between the tumor and the internal carotid artery. (**C, D**) Postoperative axial fluid-attenuated inversion recovery and coronal T1-weighted MRI images documenting the complete excision of the schwannoma. MRI, magnetic resonance imaging.

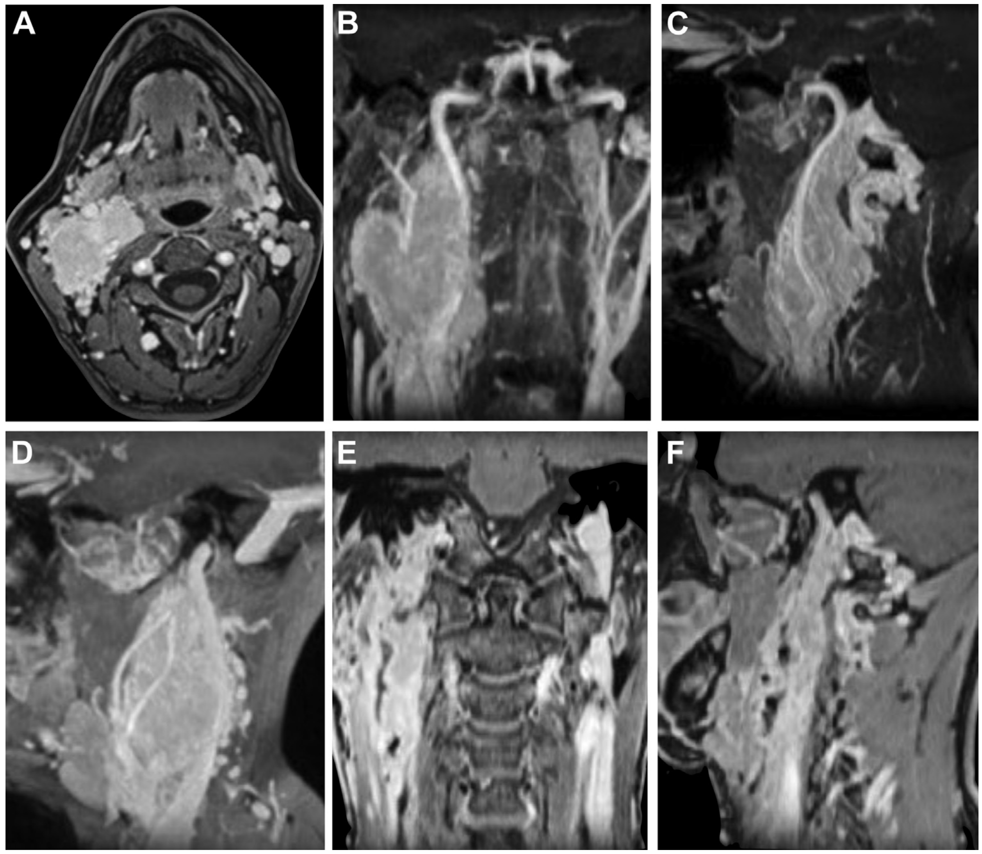

Figure 13. (**A**) Axial gadolinium contrast-enhanced T1-weighted MRI image showing a large right schwannoma involving the parapharyngeal, carotid, parotid, and prevertebral spaces. (**B**) Coronal and (**C, D**) sagittal MRI angiography revealing a partial encasement of the internal carotid artery and the internal jugular vein, the latter also being compressed and shifted posteriorly. (**E**) Postoperative coronal and (**F**) sagittal T1-weighted contrast-enhanced MRI performed at the 12-month follow-up showing the gross total removal of the tumor along with no evidence of recurrence. MRI, magnetic resonance imaging.

because of different working corridors, effectiveness in allowing a gross total tumor removal in most cases, very low morbidity, and optimal cosmetic results. About the working corridors, the versatility of the ALA has been widely demonstrated throughout the series of illustrative cases reported. About the retro-jugular corridor, for which transposition of the VA is necessary, it should be emphasized that if a meticulous subperiosteal dissection is performed that this maneuver is simple and routinely employed in other posterior approaches to the posterolateral skull base, such as the far-lateral transcondylar approach[47-49] or the transcondylar, transjugular, and transtubercular variant of the extreme-lateral approach.[50]

In order to additionally enlarge the working area for lesions having a posterior extension, a partial or complete mastoidectomy sparing the Fallopian canal can be performed during the ALA. It is followed by an infralabyrinthine dissection aimed at exposing the sigmoid sinus and the jugular bulb.

In selected instances of deep-seated tumors having intimate relationships or even encasement of the PPS, ICA, or JF structures, endoscopic assistance may offer advantages when checking for residuals. In this as in other areas, endoscopy is generally used with the same technical tips reported for other pathologies.[51-57]

An additional strength of the ALA lies in the fact that, in the case of JF dumbbell schwannomas, it may be elegantly combined with other skull base approaches to accomplish a radical excision.

In the reported series, neuromonitoring of the LCNs played a role of utmost importance in achieving a good outcome, because the surgical management of large schwannomas in this area may involve the manipulation of the main trunk of the nerve. The anesthesia protocol used for neuromonitoring was the same as has already been reported by our group for other surgical neurovascular pathologies.[58-62]

CONCLUSIONS

The ALA is effective in providing an adequate exposure of the extracranial side of the JF and retrostyloid superior PPS, with no need for hearing sacrifice, facial nerve rerouting, or infralabyrinthine bony exposure.

Based on our long-term experience, the versatility that results from the multiple working corridors, the ability to extend inferiorly for larger lesions, and the possibility of combining it with other skull base approaches suggest that the ALA is the approach of choice for most cervical LCN schwannomas.

Deep knowledge of the anatomy of the PPS and the JF region is paramount for using the ALA as well as other surgical routes to these complex areas.

REFERENCES

1. Shahinian H, Dornier C, Fisch U. Parapharyngeal space tumors: the infratemporal fossa approach. *Skull Base Surg*. 1995;5:73-81.

2. Bejjani GK, Sullivan B, Salas-Lopez E, et al. Surgical anatomy of the infratemporal fossa: the styloid diaphragm revisited. *Neurosurgery*. 1998;43: 842-852 [discussion: 852-853].

3. Das Gupta TK, Brasfield RD, Strong EW, Hajdu SI. Benign solitary schwannomas (neurilemomas). *Cancer*. 1969;24:355-366.

4. Zheng X, Guo K, Wang H, et al. Extracranial schwannoma in the carotid space: a retrospective review of 91 cases. *Head Neck*. 2017;39:42-47.

5. Malone JP, Agrawal A, Schuller DE. Safety and efficacy of transcervical resection of parapharyngeal space neoplasms. *Ann Otol Rhinol Laryngol*. 2001;110:1093-1098.

6. Chang SS, Goldenberg D, Koch WM. Transcervical approach to benign parapharyngeal space tumors. *Ann Otol Rhinol Laryngol*. 2012;121:620-624.

7. Kim SM, Paek SH, Lee JH. Infratemporal fossa approach: the modified zygomatico-transmandibular approach. *Maxillofac Plast Reconstr Surg*. 2019;41:3.

8. He H, Yang Q, Gong J, et al. Endoscopic transvestibular transmandibular approach for trigeminal schwannoma in infratemporal fossa and parapharyngeal space. *World Neurosurg*. 2018;118: 172-176.

9. Guinto G, Abello J, Molina A, et al. Zygomatic-transmandibular approach for giant tumors of the infratemporal fossa and parapharyngeal space. *Neurosurgery*. 1999;45:1385-1398.

10. Stell PM, Mansfield AO, Stoney PJ. Surgical approaches to tumors of the parapharyngeal space. *Am J Otolaryngol*. 1985;6:92-97.

11. Khafif A, Segev Y, Kaplan DM, Gil Z, Fliss DM. Surgical management of parapharyngeal space tumors: a 10-year review. *Otolaryngol Head Neck Surg*. 2005;132:401-406.

12. Hamza A, Fagan JJ, Weissman JL, Myers EN. Neurilemomas of the parapharyngeal space. *Arch Otolaryngol Head Neck Surg*. 1997;123:622-626.

13. Cohen SM, Burkey BB, Netterville JL. Surgical management of parapharyngeal space masses. *Head Neck*. 2005;27:669-675.

14. Som PM, Biller HF, Lawson W. Tumors of the parapharyngeal space: preoperative evaluation, diagnosis and surgical approaches. *Ann Otol Rhinol Laryngol Suppl*. 1981;90(Pt 4):3-15.

15. Eisele DE, Netterville JL, Hoffman HT, Gantz BJ. Parapharyngeal space masses. *Head Neck*. 1999;21: 154-159.

16. O'Malley BW, Quon H, Leonhardt FD, Chalian AA, Weinstein GS. Transoral robotic surgery for parapharyngeal space tumors. *ORL J Otorhinolaryngol Relat Spec*. 2010;72:332-336.

17. Chung HJ, Moon IS, Cho H-J, et al. Analysis of surgical approaches to skull base tumors involving the pterygopalatine and infratemporal fossa. *J Craniofac Surg*. 2019;30:589-595.

18. Carrau RL, Myers EN, Johnson JT. Management of tumors arising in the parapharyngeal space. *Laryngoscope*. 1990;100:583-589.

19. Dimitrijevic MV, Jesic SD, Mikic AA, Arsovic NA, Tomanovic NR. Parapharyngeal space tumors: 61 case reviews. *Int J Oral Maxillofac Surg*. 2010;39: 983-989.

20. Lot G, George B. Cervical neuromas with extradural components: surgical management in a series of 57 patients. *Neurosurgery*. 1997;41:813-820 [discussion: 820-822].

21. George B, Laurian C, Keravel Y, Cophignon J. Extradural and hourglass cervical neurinomas: the vertebral artery problem. *Neurosurgery*. 1985;16: 591-594.

22. George B, Lot G. Neurinomas of the first two cervical nerve roots: a series of 42 cases. *J Neurosurg*. 1995;82:917-923.

23. George B, Laurian C. Surgical approach to the whole length of the vertebral artery with special reference to the third portion. *Acta Neurochir (Wien)*. 1980;51:259-272.

24. Bruneau M, George B. Foramen magnum meningiomas: detailed surgical approaches and technical aspects at Lariboisière Hospital and review of the literature. *Neurosurg Rev*. 2008;31:19-32 [discussion: 32-33].

25. Lesoin F, Jomin M, Pellerin P, et al. Transclival transcervical approach to the upper cervical spine and clivus. *Acta Neurochir (Wien)*. 1986;80:100-104.

26. Lesoin F, Franz K, Villette L, et al. Usefulness of the bilateral anterolateral approach in operations on the cervical spine. *Surg Neurol*. 1987;27:228-232.

27. Lesoin F, Rousseaux M, Pellerin P, Villette L, Autricque A, Jomin M. [The Anterior retropharyngeal intermaxillohyoid approach and acrylic prosthesis in metastatic lesions of the upper cervical spine (C1-C2)]. *J Chir (Paris)*. 1986;123: 343-346 [in French].

28. Lesoin F, Pellerin P, Lozes G, Carini S, Jomin M. [Approach to lesions of the clivus and upper cervical spine by the retropharyngeal intermaxillohyoid route]. *Neurochirurgie*. 1985;31:65-71 [in French].

29. Abd el-Bary TH, Dujovny M, Ausman JI. Microsurgical anatomy of the atlantal part of the vertebral artery. *Surg Neurol*. 1995;44:392-400 [discussion: 400-401].

30. Lang J, ed. *Skull Base and Related Structures. An Atlas of Clinical Anatomy*. 2nd ed. Stuttgart, Germany: Schattauer; 2001.

31. Luzzi S, Elia A, Del Maestro M, et al. Dysembryoplastic neuroepithelial tumors: what you need to know. *World Neurosurg*. 2019;127:255-265.

32. Ding Y, Rong H, Wang Y, et al. Detection of germline mutations of the SMARCB1 gene in a Chinese family with intraspinal schwannomatosis. *World Neurosurg*. 2019;123:318-322.

33. Bongetta D, Zoia C, Luzzi S, et al. Neurosurgical issues of bariatric surgery: a systematic review of the literature and principles of diagnosis and treatment. *Clin Neurol Neurosurg*. 2019;176:34-40.

34. Ciappetta P, D'urso PI, Luzzi S, Ingravallo G, Cimmino A, Resta L. Cystic dilation of the ventriculus terminalis in adults. *J Neurosurg Spine*. 2008;8:92-99.

35. Bellantoni G, Guerrini F, Del Maestro M, Galzio R, Luzzi S. Simple schwannomatosis or an incomplete Coffin-Siris? Report of a particular case. *eNeurologicalSci*. 2019;14:31-33.

36. Zoia C, Bongetta D, Guerrini F, et al. Outcome of elderly patients undergoing intracranial meningioma resection: a single center experience [epub ahead of print]. *J Neurosurg Sci*. 2018. https://doi.org/10.23736/S0390-5616.18.04333-3.

37. Ding Y, Rong H, Liu T, et al. Malignant peripheral nerve sheath tumor arising in schwannomatosis with multiple lung metastases. *World Neurosurg*. 2018;119:335-339.

38. Toms J, Harrison J, Richard H, Childers A, Reiter ER, Graham RS. An unusual case of schwannomatosis with bilateral maxillary sinus schwannomas and a novel SMARCB1 gene mutation. *J Neurosurg Spine*. 2016;24:160-166.

39. De Tommasi A, Luzzi S, D'Urso PI, De Tommasi C, Resta N, Ciappetta P. Molecular genetic analysis in a case of ganglioglioma: identification of a new mutation. *Neurosurgery*. 2008;63: 976-980 [discussion: 980].

40. De Tommasi A, Occhiogrosso G, De Tommasi C, Luzzi S, Cimmino A, Ciappetta P. A polycystic variant of a primary intracranial leptomeningeal astrocytoma: case report and literature review. *World J Surg Oncol*. 2007;5:72.

41. Palumbo P, Lombardi F, Siragusa G, et al. Involvement of NOS2 activity on human glioma cell growth, clonogenic potential, and neurosphere generation. *Int J Mol Sci*. 2018;19. https://doi.org/10.3390/ijms19092801.

42. Raysi Dehcordi S, Ricci A, Di Vitantonio H, et al. Stemness marker detection in the periphery of glioblastoma and ability of glioblastoma to generate glioma stem cells: clinical correlations. *World Neurosurg*. 2017;105:895-905.

43. Luzzi S, Crovace AM, Lacitignola L, et al. Engraftment, neuroglial transdifferentiation and behavioral recovery after complete spinal cord transection in rats. *Surg Neurol Int*. 2018;9:19.

44. Palumbo P, Lombardi F, Augello FR, et al. NOS2 inhibitor 1400W induces autophagic flux and influences extracellular vesicle profile in human glioblastoma U87MG cell line. *Int J Mol Sci*. 2019; 20. https://doi.org/10.3390/ijms20123010.

45. Liao H, Hua Q, Wu Z. [Maxillary swing approach in the management of tumors in the central and lateral cranial base]. *Zhonghua Er Bi Yan Hou Tou Jing Wai Ke Za Zhi*. 2006;41:276-280 [in Chinese].

46. Prasad SC, Piccirillo E, Chovanec M, La Melia C, De Donato G, Sanna M. Lateral skull base approaches in the management of benign parapharyngeal space tumors. *Auris Nasus Larynx*. 2015; 42:189-198.

47. Wen HT, Rhoton AL, Katsuta T, de Oliveira E. Microsurgical anatomy of the transcondylar, supracondylar, and paracondylar extensions of the far-lateral approach. *J Neurosurg*. 1997;87:555-585.

48. al-Mefty O, Borba LA, Aoki N, Angtuaco E, Pait TG. The transcondylar approach to extradural nonneoplastic lesions of the craniovertebral junction. *J Neurosurg*. 1996;84:1-6.

49. Ciappetta P, Occhiogrosso G, Luzzi S, D'Urso PI, Garribba AP. Jugular tubercle and vertebral artery/posterior inferior cerebellar artery anatomic relationship: a 3-dimensional angiography computed tomography anthropometric study. *Neurosurgery*. 2009;64(Suppl 2):429-436 [discussion: 436].

50. Salas E, Sekhar LN, Ziyal IM, Caputy AJ, Wright DC. Variations of the extreme-lateral craniocervical approach: anatomical study and clinical analysis of 69 patients. *J Neurosurg*. 1999; 90(Suppl):206-219.

51. Gallieni M, Del Maestro M, Luzzi S, Trovarelli D, Ricci A, Galzio R. Endoscope-assisted microneurosurgery for intracranial aneurysms: operative technique, reliability, and feasibility based on 14 years of personal experience. *Acta Neurochir Suppl*. 2018;129:19-24.

52. Cheng C-Y, Shetty R, Sekhar LN, Luzzi S. Microsurgical resection of a large intraventricular trigonal tumor: 3-dimensional operative video (Comment). *Oper Neurosurg*. 2018;15:E92-E93.

53. Luzzi S, Elia A, Del Maestro M, et al. Indication, timing, and surgical treatment of spontaneous intracerebral hemorrhage: systematic review and proposal of a management algorithm [epub ahead of print]. *World Neurosurg*. 2019. https://doi.org/10.1016/j.wneu.2019.01.016.

54. Luzzi S, Del Maestro M, Trovarelli D, et al. Endoscope-assisted microneurosurgery for neurovascular compression syndromes: basic principles, methodology, and technical notes. *Asian J Neurosurg*. 2019;14:193-200.

55. Luzzi S, Del Maestro M, Elia A, et al. Morphometric and radiomorphometric study of the correlation between the foramen magnum region and the anterior and posterolateral approaches to ventral intradural lesions [epub ahead of print]. *Turk Neurosurg*. 2019. https://doi.org/10.5137/1019-5149.JTN.26052-19.2.

56. Zoia C, Bongetta D, Dorelli G, Luzzi S, Maestro MD, Galzio RJ. Transnasal endoscopic removal of a retrochiasmatic cavernoma: a case report and review of literature. *Surg Neurol Int*. 2019;10:76.

57. Luzzi S, Zoia C, Rampini AD, et al. Lateral transorbital neuroendoscopic approach for intraconal meningioma of the orbital apex: technical nuances and literature review. *World Neurosurg*. 2019;131:10-17.

58. Ciappetta P, Luzzi S, De Blasi R, D'Urso PI. Extracranial aneurysms of the posterior inferior cerebellar artery. Literature review and report of a new case. *J Neurosurg Sci*. 2009;53:147-151.

59. Del Maestro M, Luzzi S, Gallieni M, et al. Surgical treatment of arteriovenous malformations: role of preoperative staged embolization. *Acta Neurochir Suppl*. 2018;129:109-113.

60. Luzzi S, Del Maestro M, Bongetta D, et al. Onyx embolization before the surgical treatment of grade III Spetzler-Martin brain arteriovenous malformations: single-center experience and technical nuances. *World Neurosurg*. 2018;116: e340-e353.

61. Luzzi S, Gallieni M, Del Maestro M, Trovarelli D, Ricci A, Galzio R. Giant and very large intracranial aneurysms: surgical strategies and special issues. *Acta Neurochir Suppl*. 2018;129:25-31.

62. Ricci A, Di Vitantonio H, De Paulis D, et al. Cortical aneurysms of the middle cerebral artery: a review of the literature. *Surg Neurol Int*. 2017;8:117.

Conflict of interest statement: The authors declare that the article content was composed in the absence of any commercial or financial relationships that could be construed as a potential conflict of interest.

Received 28 July 2019; accepted 3 September 2019

Citation: World Neurosurg. (2019) 132:e40-e52.
https://doi.org/10.1016/j.wneu.2019.09.006

Journal homepage: ***www.journals.elsevier.com/world-neurosurgery***

Available online: ***www.sciencedirect.com***